Time-dependent reliability analysis by a single-loop Bayesian active learning method using Gaussian process regression

Chao Dang[a,*], Marcos A. Valdebenito[a], Matthias G.R. Faes[a,b]

[a] *Chair for Reliability Engineering, TU Dortmund University, Leonhard-Euler-Straße 5, Dortmund 44227, Germany*
[b] *International Joint Research Center for Engineering Reliability and Stochastic Mechanics, Tongji University, Shanghai 200092, China*

Abstract

Time-dependent reliability analysis has proven to be an invaluable tool for assessing the safety levels of engineering structures subject to both randomness and time-varying factors. In this context, single-loop active learning Kriging methods have demonstrated a favorable trade-off between efficiency and accuracy. However, there remains significant potential for further improvement, particularly in addressing computationally expensive time-dependent reliability problems. This paper introduces a novel single-loop Bayesian active learning method using Gaussian process regression (GPR) for time-dependent reliability analysis, termed 'Integrated Bayesian Integration and Optimization' (IBIO). The key idea is to integrate the Bayesian probabilistic integration method originally developed for static reliability analysis and the Bayesian global optimization for solving the global optima of expensive black-box functions. First, we introduce a pragmatic estimator for the time-dependent failure probability. Second, a new stopping criterion is proposed to determine when the active learning process should be terminated. Third, three learning functions as three alternatives are developed to identity the next best time instant where to evaluate the performance function. Fourth, one new learning function is presented to select the next best sample for the random variables and stochastic processes given the time instant. Five numerical examples are presented to demonstrate the effectiveness of the proposed IBIO method. It is empirically shown that the method can produce accurate results with only a small number of performance function evaluations.

Keywords: Time-dependent reliability analysis; Bayesian active learning; Gaussian process regression; Stopping criterion; Learning function

1. Introduction

Ensuring the safety of engineering structures is essential for protecting lives, preserving property, maintaining functionality, and supporting sustainable development. However, most engineering structures in operation are inevitably influenced by the combined effects of randomness and time-varying factors. For example, randomness may stem from the natural variability in material properties and loading conditions, while time-varying factors can result from corrosion, fatigue, and deterioration. As a result, time-dependent reliability analysis has proven to be an invaluable tool for evaluating the safety levels of engineering structures. Over the decades, numerous methods have been developed to advance this field of study. These existing methods can be broadly categorized into three groups: (1) out-crossing rate methods; (2) composite limit state methods; and (3) extreme value methods.

As the most classical approach, out-crossing rate methods express the time-dependent failure probability as an integral of the out-crossing rate (i.e., the rate at which a performance function crosses zero over time). This concept was first introduced by Rice [1], who developed what is now known as the Rice formula. Since then, various out-crossing rate methods have been developed for time-dependent reliability analysis, including PHI2 [2], PHI2+ [3], moment-based PHI2 (MPHI2) [4], PHI2++ [5], and many others [6–8]. However, these methods rely on the potentially unwarranted assumption that all out-crossing events are mutually independent, which can lead to significant errors when the events exhibit strong dependence. Furthermore, out-crossing rate methods often require a substantial number of performance function evaluations, rendering them computationally prohibitive for problems involving expensive-to-evaluate performance functions.

Alternatively, composite limit state methods discretize a time-dependent performance function into a sequence of instantaneous performance functions at discrete time nodes, thereby transforming a time-dependent reliability problem into a static series-system reliability problem. Examples of such methods include the first-order reliability method (FORM) [9–11], line sampling [12], importance sampling [13, 14] and subset stimulation [15]. It is well known that FORM loses accuracy in moderate and highly nonlinear

*Corresponding author
Email address: chao.dang@tu-dortmund.de (Chao Dang)

problems, while stochastic simulation methods typically require a large number of performance function evaluations to achieve convergence.

Like composite limit state methods, extreme value methods also transform a time-dependent reliability problem into a time-independent counterpart. This, however, is achieved by considering the the extreme value distribution (EVD) of the performance function with respect to time. In this context, some EVD estimation methods have been developed especially for time-dependent reliability analysis [16–18]. In addition, numerous active learning Kriging (or Gaussian process regression (GPR)) methods have also been proposed, which can be broadly categorized into: double-loop active learning Kriging methods and single-loop active learning Kriging methods. Double-loop active learning Kriging methods involve constructing an extreme response Kriging model in the outer loop, while a separate Kriging model is built in the inner loop to identify the extreme response. Representative examples in this category include the nested extreme response method [19], mixed efficient global optimization (EGO) method [20], parallel EGO method [21] and importance sampling-based double-loop Kriging method [22]. On the contrary, single-loop active learning Kriging methods directly construct a global response Kriging model for the performance function. A non-exhaustive list of such methods include the single-loop Kriging method [23], active failure-pursuing Kriging method [24], single-loop Kriging method considering the first failure instant [25], real-time estimation error-guided active learning Kriging method [26], estimation variance reduction-guided adaptive Kriging method [27], structural state classification probability reduction adaptive Kriging method [28], subdomain uncertainty-guided Kriging method [29] and single-loop GPR based-active learning method [30]. These single-loop methods have demonstrated a favorable trade-off between efficiency and accuracy in time-dependent reliability analysis. However, it is still highly desirable to further reduce the computational costs while maintaining accuracy, particularly for solving real-world time-dependent reliability problems.

To this end, this paper presents a novel single-loop Bayesian active learning method using GPR for computationally expensive time-dependent reliability analysis, which is termed 'Integrated Bayesian Integration and Optimization' (IBIO). As the name suggests, the proposed method combines the Bayesian probabilistic integration technique, originally developed for time-independent reliability analysis [31], with Bayesian

global optimization for solving the global optima of costly black-box functions [32]. The IBIO method is versatile and applicable regardless of whether stochastic processes are involved. Moreover, it provides not only the time-dependent failure probability over a specified time interval but also the evolution of the failure probability within the interval as a byproduct. The main contributions can be summarized as follows. First, we introduce a pragmatic estimator for the time-dependent failure probability which relates not only to the posterior mean function of the GPR, but also the posterior standard deviation function. Second, based on the estimator, a new stopping criterion is proposed to determine when the iterative learning should halt, which ensures that the iterative process is neither prematurely terminated nor continued unnecessarily. Third, three novel learning functions as three alternatives are proposed to identify the next best time instant where to evaluate the performance function. Fourth, one new learning function is presented to select the next best sample for the random variables and stochastic processes given the identified time instant that improves the GPR model the most.

The remainder of this paper is organized as follows. Some preliminaries are provided in Section 2. Section 3 presents the proposed IBIO method for time-dependent reliability analysis. Five numerical examples are investigated in Section 4 to demonstrate the proposed method. Finally, concluding remarks are given in Section 5.

2. Preliminaries

This section provides background information on time-dependent reliability analysis. Section 2.1 presents the formulation of the time-dependent reliability problem. This is followed by the discretization of stochastic processes in Section 2.2. Finally, the Monte Carlo Simulation (MCS) method for solving the time-dependent failure probability is discussed in Section 2.3.

2.1. Problem formulation

Let $\boldsymbol{X} = [X_1, X_2, \cdots, X_{d_1}] \in \mathcal{D}_{\boldsymbol{X}} \subseteq \mathbb{R}^{d_1}$ represent a vector of d_1 continuous random variables with support $\mathcal{D}_{\boldsymbol{X}}$, defined on the probability space $(\Omega_{\boldsymbol{X}}, \mathcal{F}_{\boldsymbol{X}}, \mathcal{P}_{\boldsymbol{X}})$, where $\Omega_{\boldsymbol{X}}$ is the sample space, $\mathcal{F}_{\boldsymbol{X}}$ is the σ-algebra of measurable events and $\mathcal{P}_{\boldsymbol{X}}$ is the probability measure. Similarly, let $\boldsymbol{Y}(t) = [Y_1(t), Y_2(t), \cdots, Y_{d_2}(t)] \in$

$\mathcal{D}_{\boldsymbol{Y}} \subseteq \mathbb{R}^{d_2}$ denote a vector of d_2 continuous-time stochastic processes with support $\mathcal{D}_{\boldsymbol{Y}}$ (t is the time parameter), defined on the probability space $(\Omega_{\boldsymbol{Y}}, \mathcal{F}_{\boldsymbol{Y}}, \mathcal{P}_{\boldsymbol{Y}})$. In this work, the vector of stochastic processes will also be expressed as $\boldsymbol{Y}(\omega_{\boldsymbol{Y}}, t)$ if desired, where $\omega_{\boldsymbol{Y}} \in \Omega_{\boldsymbol{Y}}$, emphasizing that $\boldsymbol{Y}$ is actually a function of both $\omega_{\boldsymbol{Y}}$ and t. Consider the performance function (also known as the limit state function) $g(\boldsymbol{X}, \boldsymbol{Y}(t), t)$, where $t \in [t_0, t_f]$ represents the time period of interest. By convention, failure occurs when g takes a negative value at any time within $[t_0, t_f]$. The corresponding time-dependent failure probability is formally defined as:

$$P_f(t_0, t_f) = \mathbb{P}\left\{g(\boldsymbol{X}, \boldsymbol{Y}(t), t) < 0, \exists t \in [t_0, t_f]\right\}, \tag{1}$$

where $\mathbb{P}$ is the probability operator, and $\exists$ means 'there exists'. The so-called time-dependent reliability $R(t_0, t_f)$ is the complement of $P_f(t_0, t_f)$, i.e., $R(t_0, t_f) = 1 - P_f(t_0, t_f)$. By considering the minimum value of $g(\boldsymbol{X}, \boldsymbol{Y}(t), t)$ over the interval $[t_0, t_f]$, the time-dependent failure probability $P_f(t_0, t_f)$, as defined in Eq. (1), is equivalent to:

$$\begin{aligned} P_f(t_0, t_f) =& \mathbb{P}\left\{\min_{t\in[t_0,t_f]} g(\boldsymbol{X}, \boldsymbol{Y}(t), t) < 0\right\} \\ =& \int_{\mathcal{D}_{\boldsymbol{X}}} \int_{\Omega_{\boldsymbol{Y}}} I\left(\min_{t\in[t_0,t_f]} g(\boldsymbol{x}, \boldsymbol{y}(\omega_{\boldsymbol{Y}}, t), t) < 0\right) f_{\boldsymbol{X}}(\boldsymbol{x}) \mathrm{d}\boldsymbol{x} \mathrm{d}\mathbb{P}\left(\omega_{\boldsymbol{Y}}\right) \\ =& \int_{\mathcal{D}_{\boldsymbol{X}}} \int_{\Omega_{\boldsymbol{Y}}} \max_{t\in[t_0,t_f]} I\left(g(\boldsymbol{x}, \boldsymbol{y}(\omega_{\boldsymbol{Y}}, t), t) < 0\right) f_{\boldsymbol{X}}(\boldsymbol{x}) \mathrm{d}\boldsymbol{x} \mathrm{d}\mathbb{P}\left(\omega_{\boldsymbol{Y}}\right), \end{aligned} \tag{2}$$

where $I(\cdot)$ is the indicator function: it returns one if its argument is true, and zero otherwise; $f_{\boldsymbol{X}}(\boldsymbol{x})$ is the joint probability density function (PDF) of $\boldsymbol{X}$. The equivalence between the second and final lines of Eq. (2) is straightforward, but the second-line form is far more common in the literature while the final form seldom appears. We include the latter here to facilitate later developments.

2.2. Discretization of stochastic processes

For computational purposes, the input stochastic processes input to the performance function need to be discretized. In this context, numerous well-established techniques are available in the literature, including Karhunen–Loève (KL) expansion [33], expansion optimal linear estimation [34], orthogonal series expansion [35], spectral representation [36], among many others. For the proposed method presented in Section 3, there are in principle no limitations on the types of stochastic processes and the methods used to discretize

them. However, for illustration purposes, we only consider a second-order (i.e., square-integrable) stochastic process $Y(t)$ and employ the KL expansion as an example. Let $\mu(t)$, $c(t_1, t_2)$ denote the mean and covariance functions of $Y(t)$, respectively. The time interval $[t_0, t_f]$ is first discretized into n_t equally spaced time points, i.e., $t_0, t_1, \cdots, t_{n_t-2}, t_{n_t-1} = t_f$. A truncated KL expansion of $Y(t)$ is given by:

$$\widehat{Y}(t) = \mu(t) + \sum_{j=1}^{p} \sqrt{\lambda_j} \xi_j \varphi_j(t), t = t_0, t_1, \cdots, t_{n_t-1}, \tag{3}$$

where λ_j is the j-th dominate eigenvalue of the covariance matrix $\boldsymbol{C} = [c(t_{i_1}, t_{i_2})]$ (i.e., $\lambda_1 > \lambda_2 > \cdots > \lambda_{n_t}$) and $\varphi_j(t)$ is the corresponding eigenfunction; $\{\xi_j\}_{j=1}^{p}$ is a set of p uncorrelated standardized random variables; p is the number of truncation terms, which can be determined by the approximate explained variance ratio:

$$p = \underset{p \in [1,2,\cdots,n_t]}{\arg\min} \left\{ \frac{\sum_{j=1}^{p} \lambda_i}{\sum_{j=1}^{n_t} \lambda_i} \geq \delta \right\}, \tag{4}$$

where $\delta \in (0, 1]$ is a user-defined threshold. A larger δ retains more of the process variance but requires more random variables to represent the stochastic process. Common choices in the literature are $\delta = 0.95$ or 0.99.

2.3. Time-dependent reliability analysis by MCS

The time-dependent failure probability defined early can be solved by using the crude MCS. The estimator of $P_f(t_0, t_f)$ is given by:

$$\hat{P}_f(t_0, t_f) = \frac{1}{N} \sum_{s=1}^{N} I \left(\min_{i=0,1,\cdots,n_t-1} g(\boldsymbol{x}^{(s)}, \hat{\boldsymbol{y}}^{(s)}(t_i), t_i) < 0 \right), \tag{5}$$

where $\left\{\boldsymbol{x}^{(s)}\right\}_{s=1}^{N}$ is a set of N random samples of $\boldsymbol{X}$; $\left\{\hat{\boldsymbol{y}}^{(s)}(t_i)\right\}_{s=1}^{N}$ is a set of N random samples of $\boldsymbol{Y}(t_i)$ generated, for example, by using the KL expansion. The associated coefficient of variation (CoV) is expressed as:

$$\mathrm{CoV}\left[\hat{P}_f(t_0, t_f)\right] = \sqrt{\frac{1 - \hat{P}_f(t_0, t_f)}{(N-1)\hat{P}_f(t_0, t_f)}}. \tag{6}$$

The crude MCS offers a robust tool for estimating the time-dependent failure probability. However, it requires a total of $N \times n_t$ evaluations of the performance function g, which can be computationally prohibitive when each evaluation is time-consuming, as is often the case in practice.

3. Proposed IBIO method

In this section, the proposed IBIO method is introduced for time-dependent reliability analysis. Section 3.1 provides an overview of the method. The time-dependent failure probability estimator, stopping criterion and learning functions are presented in Sections 3.2, 3.3 and 3.4, respectively. Finally, the procedure for implementing the proposed method is outlined in Section 3.5.

3.1. Overview of the proposed method

The core idea of the proposed IBIO method is to iteratively refine a GPR model of the performance function (as described in Appendix A) until the predicted time-dependent failure probability achieves a desired level of accuracy. Starting with an initial set of training data, the method builds a probabilistic surrogate model for the performance function using GPR to predict the time-dependent failure probability. If a stopping criterion is not met, a new point is selected using a learning function, and the corresponding output of g is obtained and the training data is enriched. This updated dataset is then used to refine the GPR model in the next iteration. The process repeats until the stopping criterion is satisfied. The general workflow of the proposed method is shown in Fig. 1, with some notations explained in Appendix A.

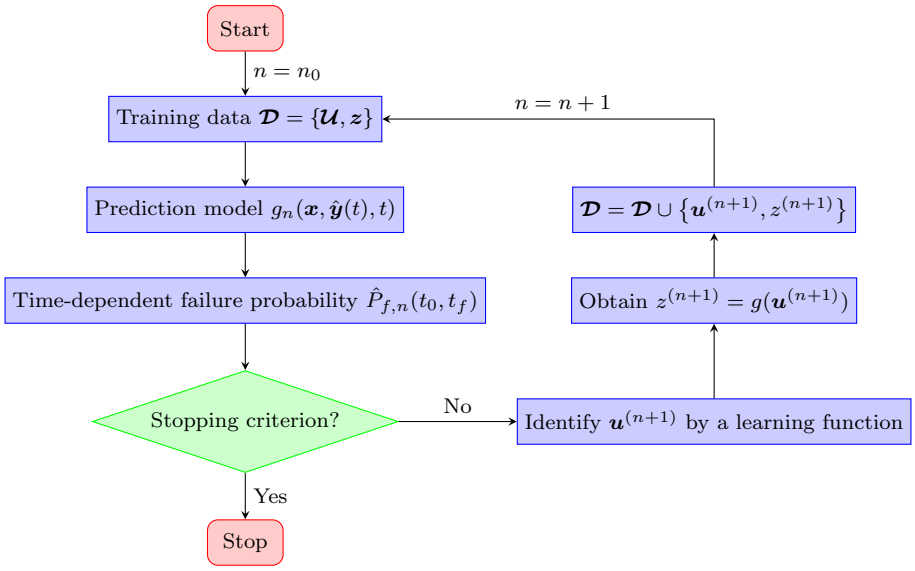

Figure 1: General workflow of the proposed IBIO method.

3.2. Time-dependent failure probability estimator

Assuming a GPR-based prediction model g_n has been constructed for the performance function g (see Appendix A), the next step is to evaluate the time-dependent failure probability using this model. This requires formulating an estimator for the time-dependent failure probability. A straightforward approach, commonly adopted in existing methods, is to use the posterior mean function, m_n, as a substitute of g to predict the time-dependent failure probability. In this study, however, an alternative approach is proposed as introduced below.

According to the previous studies on time-independent reliability analysis [37–39], the posterior mean function of I can be obtained as:

$$m_{I_n}(\boldsymbol{x}, \hat{\boldsymbol{y}}(t_i), t_i) = \Phi\left(-\frac{m_{g_n}(\boldsymbol{x}, \hat{\boldsymbol{y}}(t_i), t_i)}{\sigma_{g_n}(\boldsymbol{x}, \hat{\boldsymbol{y}}(t_i), t_i)}\right), i = 0, 1, \cdots, n_t - 1, \tag{7}$$

where I_n denotes the posterior distribution of the indicator function I; Φ is the cumulative distribution function of the standard normal variable; m_{g_n} and σ_{g_n} are the posterior mean and standard deviation functions of g, respectively.

By replacing the indicator function I in Eq. (2) with its posterior mean function m_{I_n} in Eq. (7), we can obtain an alternative estimator for time-dependent failure probability:

$$P_{f,n}(t_0, t_f) = \int_{\mathcal{D}_{\boldsymbol{X}}} \int_{\Omega_{\boldsymbol{Y}}} \max_{i=0}^{n_t-1} \Phi\left(-\frac{m_{g_n}(\boldsymbol{x}, \hat{\boldsymbol{y}}(\omega_{\boldsymbol{Y}}, t_i), t_i)}{\sigma_{g_n}(\boldsymbol{x}, \hat{\boldsymbol{y}}(\omega_{\boldsymbol{Y}}, t_i), t_i)}\right) f_{\boldsymbol{X}}(\boldsymbol{x}) \mathrm{d}\boldsymbol{x} \mathrm{d}\mathbb{P}(\omega_{\boldsymbol{Y}}). \tag{8}$$

It should be noted that if $n_t \to \infty$ and $\sigma_{g_n} \to 0$, $P_{f,n}(t_0, t_f)$ theoretically approaches to $P_f(t_0, t_f)$. Similar estimators have been developed in slightly different contexts or from different perspectives in [40, 41]. Due to the analytical intractability, the estimator of the time-dependent failure probability, as defined in Eq. (8), necessitates numerical or analytical approximation in practice. In this study, we employ the MCS method due to its simplicity and robustness.

The MCS estimator of $P_{f,n}(t_0, t_f)$ is given by:

$$\hat{P}_{f,n}(t_0, t_f) = \frac{1}{N} \sum_{j=1}^{N} \max_{i=0}^{n_t-1} \Phi\left(-\frac{m_{g_n}(\boldsymbol{x}^{(j)}, \hat{\boldsymbol{y}}^{(j)}(t_i), t_i)}{\sigma_{g_n}(\boldsymbol{x}^{(j)}, \hat{\boldsymbol{y}}^{(j)}(t_i), t_i)}\right), \tag{9}$$

where $\left\{\boldsymbol{x}^{(j)}\right\}_{j=1}^{N}$ is a set of N random samples generated according to $f_{\boldsymbol{X}}(\boldsymbol{x})$; $\left\{\hat{\boldsymbol{y}}^{(j)}(t_i)\right\}_{j=1}^{N}$ at a given i represents N random samples of $\widehat{\boldsymbol{Y}}(t_i)$. The associated variance is expressed as:

$$\mathrm{Var}\left[\hat{P}_{f,n}(t_0,t_f)\right]=\frac{1}{N(N-1)}\sum_{j=1}^{N}\left[\max_{i=0}^{n_t-1}\Phi\left(-\frac{m_{g_n}(\boldsymbol{x}^{(j)},\hat{\boldsymbol{y}}^{(j)}(t_i),t_i)}{\sigma_{g_n}(\boldsymbol{x}^{(j)},\hat{\boldsymbol{y}}^{(j)}(t_i),t_i)}\right)-\hat{P}_{f,n}(t_0,t_f)\right]^2. \tag{10}$$

3.3. Stopping criterion

Having obtained the time-dependent failure probability estimate, a stopping criterion is required to assess whether the estimate reaches a desired level of accuracy. In fact, a well-defined stopping criterion is crucial for the overall efficiency and accuracy of an active learning time-dependent reliability analysis method. In this study, we also propose a new stopping criterion.

If we replace the term m_{g_n} in Eq. (8) with the lower and upper credible bounds of g, then we can have another two quantities:

$$\begin{aligned}P^{+}_{f,n}(t_0,t_f)&=\int_{\mathcal{D}_{\boldsymbol{X}}}\int_{\Omega_{\boldsymbol{Y}}}\max_{i=0}^{n_t-1}\Phi\left(-\frac{m_{g_n}(\boldsymbol{x},\hat{\boldsymbol{y}}(\omega_{\boldsymbol{Y}},t_i),t_i)-b\sigma_{g_n}(\boldsymbol{x},\hat{\boldsymbol{y}}(\omega_{\boldsymbol{Y}},t_i),t_i)}{\sigma_{g_n}(\boldsymbol{x},\hat{\boldsymbol{y}}(\omega_{\boldsymbol{Y}},t_i),t_i)}\right)f_{\boldsymbol{X}}(\boldsymbol{x})\mathrm{d}\boldsymbol{x}\mathrm{d}\mathbb{P}(\omega_{\boldsymbol{Y}})\\&=\int_{\mathcal{D}_{\boldsymbol{X}}}\int_{\Omega_{\boldsymbol{Y}}}\max_{i=0}^{n_t-1}\Phi\left(-\frac{m_{g_n}(\boldsymbol{x},\hat{\boldsymbol{y}}(\omega_{\boldsymbol{Y}},t_i),t_i)}{\sigma_{g_n}(\boldsymbol{x},\hat{\boldsymbol{y}}(\omega_{\boldsymbol{Y}},t_i),t_i)}+b\right)f_{\boldsymbol{X}}(\boldsymbol{x})\mathrm{d}\boldsymbol{x}\mathrm{d}\mathbb{P}(\omega_{\boldsymbol{Y}}),\end{aligned} \tag{11}$$

$$\begin{aligned}P^{-}_{f,n}(t_0,t_f)&=\int_{\mathcal{D}_{\boldsymbol{X}}}\int_{\Omega_{\boldsymbol{Y}}}\max_{i=0}^{n_t-1}\Phi\left(-\frac{m_{g_n}(\boldsymbol{x},\hat{\boldsymbol{y}}(\omega_{\boldsymbol{Y}},t_i),t_i)+b\sigma_{g_n}(\boldsymbol{x},\hat{\boldsymbol{y}}(\omega_{\boldsymbol{Y}},t_i),t_i)}{\sigma_{g_n}(\boldsymbol{x},\hat{\boldsymbol{y}}(\omega_{\boldsymbol{Y}},t_i),t_i)}\right)f_{\boldsymbol{X}}(\boldsymbol{x})\mathrm{d}\boldsymbol{x}\mathrm{d}\mathbb{P}(\omega_{\boldsymbol{Y}})\\&=\int_{\mathcal{D}_{\boldsymbol{X}}}\int_{\Omega_{\boldsymbol{Y}}}\max_{i=0}^{n_t-1}\Phi\left(-\frac{m_{g_n}(\boldsymbol{x},\hat{\boldsymbol{y}}(\omega_{\boldsymbol{Y}},t_i),t_i)}{\sigma_{g_n}(\boldsymbol{x},\hat{\boldsymbol{y}}(\omega_{\boldsymbol{Y}},t_i),t_i)}-b\right)f_{\boldsymbol{X}}(\boldsymbol{x})\mathrm{d}\boldsymbol{x}\mathrm{d}\mathbb{P}(\omega_{\boldsymbol{Y}}),\end{aligned} \tag{12}$$

where $b>0$ is the credibility parameter corresponding to a $(1-\alpha)\times100\%$ credible level, i.e., $b=\Phi^{-1}(1-\alpha/2)$. It is straightforward to prove that $P^{-}_{f,n}(t_0,t_f)<P_{f,n}(t_0,t_f)<P^{+}_{f,n}(t_0,t_f)$ holds. Therefore, $P^{-}_{f,n}(t_0,t_f)$ and $P^{+}_{f,n}(t_0,t_f)$ can be interpreted as, respectively, an optimistic and a conservative estimator of the time-dependent failure probability, in contrast to the nominal estimator $P_{f,n}(t_0,t_f)$. Furthermore, as $\sigma_{g_n}\to0$, $P^{-}_{f,n}(t_0,t_f)\to P_{f,n}(t_0,t_f)$ and $P^{+}_{f,n}(t_0,t_f)\to P_{f,n}(t_0,t_f)$.

The proposed stopping criterion is defined as follows:

$$\frac{P^{+}_{f,n}(t_0,t_f)-P^{-}_{f,n}(t_0,t_f)}{P_{f,n}(t_0,t_f)}<\epsilon_3, \tag{13}$$

where ϵ_3 is a user-specified threshold. This criterion terminates the iterative process when the relative difference between the conservative failure probability estimate $P^{+}_{f,n}(t_0,t_f)$ and the optimistic estimate

$P^{-}_{f,n}(t_0, t_f)$ falls below ϵ_3, indicating that further iterations provide negligible improvement to the solution. As a side note, the proposed stopping criterion can be seen as an extension of Stopping Criterion 3 in [31], generalizing it from time-independent to time-dependent reliability analysis. Similar to $P_{f,n}(t_0, t_f)$, $P^{+}_{f,n}(t_0, t_f)$ and $P^{-}_{f,n}(t_0, t_f)$ are also evaluated using MCS in this study.

Remark 1. In a manner similar to the stopping criterion in Ineq. (13), we can also define the following two stopping criteria:

$$\frac{P_{f,n}(t_0, t_f) - P^{-}_{f,n}(t_0, t_f)}{P_{f,n}(t_0, t_f)} < \epsilon_1, \tag{14}$$

$$\frac{P^{+}_{f,n}(t_0, t_f) - P_{f,n}(t_0, t_f)}{P_{f,n}(t_0, t_f)} < \epsilon_2, \tag{15}$$

where ϵ_1 and ϵ_2 are two user-specified thresholds. These criteria extend stopping criteria 1 and 2 from [31], respectively. However, only the criterion in Ineq. (13) is considered in this work, in order to avoid an overly lengthy paper.

3.4. Learning functions

If the stopping criterion is not satisfied, a learning function is needed to guide the selection of the optimal next point for evaluating the true performance function. This process further refines the GPR-based prediction model for the performance function, as well as the predicted time-dependent failure probability. Therefore, an effective learning function is essential for an active learning method in time-dependent reliability analysis. To this end, we also develop novel learning functions in this work, guided by the principle of considering the so-called minimum time (that is, the time at which the performance function attains its minimum) within the reference time interval in an average sense. Specifically, the best next point (denoted as $\left\{\boldsymbol{x}^{(n+1)}, \hat{\boldsymbol{y}}^{(n+1)}(t^{(n+1)}), t^{(n+1)}\right\}$) is identified through a two-step procedure: (1) First, the optimal next time instant $t^{(n+1)}$ is selected by a learning function; (2) Then, the next best point $\left\{\boldsymbol{x}^{(n+1)}, \hat{\boldsymbol{y}}^{(n+1)}(t^{(n+1)})\right\}$ is determined by an another learning function. The first task is based on Bayesian optimization [42], where three commonly used learning functions are explored. The objective of this task is to determine the time instant at which the performance function reaches its minimum value. However, this is done in an average sense to account for the inherent randomness associated with $\boldsymbol{X}$ and $\hat{\boldsymbol{Y}}(t)$. It is expected that the identified

time instant will be significant for estimating the time dependent failure probability $P_f(t_0, t_f)$. The second task leverages the Bayesian probabilistic integration method for time-independent reliability analysis [31]. The primary objective of this task is to identify a set of $\boldsymbol{x}$ and $\hat{\boldsymbol{y}}$ for the fixed time instant determined in the first task, thereby enhancing our understanding of the performance function at that specific time and and its vicinity.

In Bayesian optimization, three well-known learning functions are the lower confidence bound (upper confidence bound in the context of maximization), probability of improvement (PI) and expected improvement (EI) [32]. However, these notions may not be directly applicable in our case, as our problem is not a pure optimization task. Therefore, special treatment is required, as will be described below.

The lower credible bound (LCB) function of g_n is given by:

$$\mathrm{LCB}\left(\boldsymbol{X}, \hat{\boldsymbol{Y}}(t_i), t_i\right) = m_{g_n}(\boldsymbol{X}, \hat{\boldsymbol{Y}}(\omega_{\boldsymbol{Y}}, t_i), t_i) - b\sigma_{g_n}(\boldsymbol{X}, \hat{\boldsymbol{Y}}(\omega_{\boldsymbol{Y}}, t_i), t_i). \tag{16}$$

where the credibility parameter b trades off exploitation against exploration. This expression is actually a stochastic process. In case where $\boldsymbol{X} = \boldsymbol{x}$ and $\hat{\boldsymbol{Y}}(t_i) = \hat{\boldsymbol{y}}(t_i)$, the LCB function reduces to a function with respect to only t_i, $i = 0, 1, \ldots, n_t - 1$. If the goal would be to find the minimum value of $g(\boldsymbol{x}, \hat{\boldsymbol{y}}(t_i), t_i)$, the best next time instant $t^{(n+1)}$ can be chosen by minimizing $\mathrm{LCB}\left(\boldsymbol{x}, \hat{\boldsymbol{y}}(t_i), t_i\right)$. However, this is not the objective here. For our case, we further define the integrated LCB (ILCB) function by integrating out $\boldsymbol{X}$ and $\hat{\boldsymbol{Y}}(t_i)$ from the LCB function:

$$\mathrm{ILCB}(t_i) = \int_{\mathcal{D}_{\boldsymbol{X}}} \int_{\Omega_{\boldsymbol{Y}}} \left[m_{g_n}(\boldsymbol{x}, \hat{\boldsymbol{y}}(\omega_{\boldsymbol{Y}}, t_i), t_i) - b\sigma_{g_n}(\boldsymbol{x}, \hat{\boldsymbol{y}}(\omega_{\boldsymbol{Y}}, t_i), t_i)\right] f_{\boldsymbol{X}}(\boldsymbol{x}) \mathrm{d}\boldsymbol{x} \mathrm{d}\mathbb{P}\left(\omega_{\boldsymbol{Y}}\right). \tag{17}$$

The ILCB can be approximated by MCS such that:

$$\widehat{\mathrm{ILCB}}(t_i) = \frac{1}{N} \sum_{j=1}^{N} \left[m_{g_n}(\boldsymbol{x}^{(j)}, \hat{\boldsymbol{y}}^{(j)}(t_i), t_i) - b\sigma_{g_n}(\boldsymbol{x}^{(j)}, \hat{\boldsymbol{y}}^{(j)}(t_i), t_i)\right]. \tag{18}$$

The best next time instant can be selected by minimizing the $\widehat{\mathrm{ILCB}}$ such that:

$$t^{(n+1)} = \underset{t_i \in [t_0, t_1, \cdots, t_{n_t - 1}]}{\arg\min} \widehat{\mathrm{ILCB}}(t_i). \tag{19}$$

Alternatively, we can define the PI:

$$\mathrm{PI}\left(\boldsymbol{X}, \hat{\boldsymbol{Y}}(t_i), t_i\right) = \Phi\left(\frac{z_{\min} - m_{g_n}(\boldsymbol{X}, \hat{\boldsymbol{Y}}(\omega_{\boldsymbol{Y}}, t_i), t_i)}{\sigma_{g_n}(\boldsymbol{X}, \hat{\boldsymbol{Y}}(\omega_{\boldsymbol{Y}}, t_i), t_i)}\right), \tag{20}$$

where $z_{\min}$ is the minimum value of Z observed so far, i.e., $z_{\min} = \min_{i=1}^{n} z^{(i)}$. The PI function is known to be inherently exploitative. Taking the expectation of PI gives the integrated PI (IPI):

$$\mathrm{IPI}(t_i) = \int_{\mathcal{D}_{\boldsymbol{X}}} \int_{\Omega_{\boldsymbol{Y}}} \Phi\left(\frac{z_{\min} - m_{g_n}(\boldsymbol{x}, \hat{\boldsymbol{y}}(\omega_{\boldsymbol{Y}}, t_i), t_i)}{\sigma_{g_n}(\boldsymbol{x}, \hat{\boldsymbol{y}}(\omega_{\boldsymbol{Y}}, t_i), t_i)}\right) f_{\boldsymbol{X}}(\boldsymbol{x}) \mathrm{d}\boldsymbol{x} \mathrm{d}\mathbb{P}\left(\omega_{\boldsymbol{Y}}\right). \tag{21}$$

Similar to LCB, IPI can also be approximated by MCS, which is denoted as $\widehat{\mathrm{IPI}}$. Based on $\widehat{\mathrm{IPI}}$, the next best time instant is selected by:

$$t^{(n+1)} = \underset{t_i \in [t_0, t_1, \cdots, t_{n_t - 1}]}{\arg\max} \widehat{\mathrm{IPI}}(t_i). \tag{22}$$

In addition to LCB and PI, another option is the EI:

$$\begin{aligned} \mathrm{EI}\left(\boldsymbol{X}, \hat{\boldsymbol{Y}}(t_i), t_i\right) = & \left(z_{\min} - m_{g_n}(\boldsymbol{X}, \hat{\boldsymbol{Y}}(\omega_{\boldsymbol{Y}}, t_i), t_i)\right) \Phi\left(\frac{z_{\min} - m_{g_n}(\boldsymbol{X}, \hat{\boldsymbol{Y}}(\omega_{\boldsymbol{Y}}, t_i), t_i)}{\sigma_{g_n}(\boldsymbol{X}, \hat{\boldsymbol{Y}}(\omega_{\boldsymbol{Y}}, t_i), t_i)}\right) \\ & + \sigma_{g_n}(\boldsymbol{X}, \hat{\boldsymbol{Y}}(\omega_{\boldsymbol{Y}}, t_i), t_i) \phi\left(\frac{z_{\min} - m_{g_n}(\boldsymbol{X}, \hat{\boldsymbol{Y}}(\omega_{\boldsymbol{Y}}, t_i), t_i)}{\sigma_{g_n}(\boldsymbol{X}, \hat{\boldsymbol{Y}}(\omega_{\boldsymbol{Y}}, t_i), t_i)}\right), \end{aligned} \tag{23}$$

where ϕ represents the PDF of the standard normal variable. The EI function can strike a balance between exploitation and exploration by the two additive terms. Further, we can define the integrated EI (IEI):

$$\mathrm{IEI}(t_i) = \int_{\mathcal{D}_{\boldsymbol{X}}} \int_{\Omega_{\boldsymbol{Y}}} \mathrm{EI}\left(\boldsymbol{x}, \hat{\boldsymbol{y}}(\omega_{\boldsymbol{Y}}, t_i), t_i\right) f_{\boldsymbol{X}}(\boldsymbol{x}) \mathrm{d}\boldsymbol{x} \mathrm{d}\mathbb{P}\left(\omega_{\boldsymbol{Y}}\right). \tag{24}$$

The MCS is used to approximate IEI, which is denoted as $\widehat{\mathrm{IEI}}$. On this basis, the next best time instant is determined by:

$$t^{(n+1)} = \underset{t_i \in [t_0, t_1, \cdots, t_{n_t - 1}]}{\arg\max} \widehat{\mathrm{IEI}}(t_i). \tag{25}$$

These ILCB, IPI, and IEI criteria can be interpreted as identifying the next promising time instant based on the well-established LCB, PI, and EI criteria, but in an average sense. While they offer three options, their performance may vary across different problems, which will be analyzed using four numerical examples in Section 4.

After $t^{(n+1)}$ is obtained, a learning function needs to be defined to identify $\left\{\boldsymbol{x}^{(n+1)}, \hat{\boldsymbol{y}}^{(n+1)}(t^{(n+1)})\right\}$. With the time instant fixed, this can be treated analogously to a time-independent reliability problem. The following learning function is then proposed:

$$L_3(\boldsymbol{x}, \hat{\boldsymbol{y}}(t^{(n+1)})) = \left[\Phi\left(-\frac{m_{g_n}(\boldsymbol{x}, \hat{\boldsymbol{y}}(t^{(n+1)}), t^{(n+1)})}{\sigma_{g_n}(\boldsymbol{x}, \hat{\boldsymbol{y}}(t^{(n+1)}), t^{(n+1)})} + b\right) - \Phi\left(-\frac{m_{g_n}(\boldsymbol{x}, \hat{\boldsymbol{y}}(t^{(n+1)}), t^{(n+1)})}{\sigma_{g_n}(\boldsymbol{x}, \hat{\boldsymbol{y}}(t^{(n+1)}), t^{(n+1)})} - b\right)\right] f_{\boldsymbol{X}}(\boldsymbol{x}) f_{\hat{\boldsymbol{Y}}(t)}(\hat{\boldsymbol{y}}(t^{(n+1)})). \tag{26}$$

This function is derived from the integrand of $P^{+}_{f,n}(t_0,t_f) - P^{-}_{f,n}(t_0,t_f)$ by omitting the max operator and conditional on $t_i = t^{(n+1)}$. It is worth mentioning that L_3 can been seen as an adaption of the third learning function proposed in [31] originally developed for time-independent reliability analysis. The next best point $\left\{\boldsymbol{x}^{(n+1)}, \hat{\boldsymbol{y}}^{(n+1)}(t^{(n+1)})\right\}$ is identified by:

$$\left\{\boldsymbol{x}^{(n+1)}, \hat{\boldsymbol{y}}^{(n+1)}(t^{(n+1)})\right\} = \underset{j=1,2,\cdots,N}{\arg\max}\, L_3(\boldsymbol{x}^{(j)}, \hat{\boldsymbol{y}}^{(j)}(t^{(n+1)})). \tag{27}$$

Remark 2. For consistency, if the stopping criterion in Ineq. (14) is used, the following learning function should be used:

$$L_1(\boldsymbol{x}, \hat{\boldsymbol{y}}(t^{(n+1)})) = \left[\Phi\left(-\frac{m_{g_n}(\boldsymbol{x}, \hat{\boldsymbol{y}}(t^{(n+1)}), t^{(n+1)})}{\sigma_{g_n}(\boldsymbol{x}, \hat{\boldsymbol{y}}(t^{(n+1)}), t^{(n+1)})}\right) - \Phi\left(-\frac{m_{g_n}(\boldsymbol{x}, \hat{\boldsymbol{y}}(t^{(n+1)}), t^{(n+1)})}{\sigma_{g_n}(\boldsymbol{x}, \hat{\boldsymbol{y}}(t^{(n+1)}), t^{(n+1)})} - b\right)\right] f_{\boldsymbol{X}}(\boldsymbol{x}) f_{\hat{\boldsymbol{Y}}(t)}(\hat{\boldsymbol{y}}(t^{(n+1)})). \tag{28}$$

If the stopping criterion in Ineq. (15) is used, the following learning function should be used:

$$L_2(\boldsymbol{x}, \hat{\boldsymbol{y}}(t^{(n+1)})) = \left[\Phi\left(-\frac{m_{g_n}(\boldsymbol{x}, \hat{\boldsymbol{y}}(t^{(n+1)}), t^{(n+1)})}{\sigma_{g_n}(\boldsymbol{x}, \hat{\boldsymbol{y}}(t^{(n+1)}), t^{(n+1)})} + b\right) - \Phi\left(-\frac{m_{g_n}(\boldsymbol{x}, \hat{\boldsymbol{y}}(t^{(n+1)}), t^{(n+1)})}{\sigma_{g_n}(\boldsymbol{x}, \hat{\boldsymbol{y}}(t^{(n+1)}), t^{(n+1)})}\right)\right] f_{\boldsymbol{X}}(\boldsymbol{x}) f_{\hat{\boldsymbol{Y}}(t)}(\hat{\boldsymbol{y}}(t^{(n+1)})). \tag{29}$$

The functions L_1 and L_2 can be regarded as extensions of the first and second learning functions in [31], respectively.

3.5. Implementation procedure of the proposed method

The implementation procedure of the proposed IBIO method is summarized below, alongside a flowchart in Fig. 2.

Step 1: Discretize the time period

Discretize the time period $[t_0, t_f]$ into n_t equally spaced time points $t_i = t_0 + i\Delta t$ for $i = 0, 1, \cdots, n_t - 1$, with $\Delta t = \frac{t_f - t_0}{n_t - 1}$.

Step 2: Generate an initial sample pool

Generate an initial sample pool $\boldsymbol{S} = \left\{\boldsymbol{x}^{(j)}, \hat{\boldsymbol{y}}^{(j)}(t_i), t_i\right\}$ for $i = 0, 1, \cdots, n_t - 1$ and $j = 1, 2, \cdots, N$, where $\boldsymbol{x}^{(j)}$ is sampled randomly according to $f_{\boldsymbol{X}}(\boldsymbol{x})$, and $\hat{\boldsymbol{y}}^{(j)}(t_i)$ is generated randomly using the KL expansion.

Step 3: Form an initial training dataset

Form a small initial training dataset $\boldsymbol{\mathcal{D}} = \{\boldsymbol{\mathcal{U}}, \boldsymbol{z}\}$, where $\boldsymbol{\mathcal{U}} = \left\{\boldsymbol{\mathcal{X}}, \hat{\boldsymbol{\mathcal{Y}}}(\boldsymbol{t}), \boldsymbol{t}\right\} = \left\{\boldsymbol{x}^{(j)}, \hat{\boldsymbol{y}}^{(j)}(t_j), t_j\right\}_{j=1}^{n_0}$ and $\boldsymbol{z} = \left\{g(\boldsymbol{x}^{(j)}, \hat{\boldsymbol{y}}^{(j)}(t_j), t_j)\right\}_{j=1}^{n_0}$. Here, $\boldsymbol{t} = \{t_j\}_{j=1}^{n_0}$ is a vector of n_0 equally spaced time instants over $[t_0, t_f]$, $\boldsymbol{\mathcal{X}} = \left\{\boldsymbol{x}^{(j)}\right\}_{j=1}^{n_0}$ contains n_0 samples of $\boldsymbol{X}$ generated using the Hammersley point set, and $\hat{\boldsymbol{\mathcal{Y}}}(\boldsymbol{t}) = \left\{\hat{\boldsymbol{y}}^{(j)}(t_j)\right\}_{j=1}^{n_0}$ is generated by KL expansion with the Hammersley point set. Let $n = n_0$.

Step 4: Construct a GPR model

Construct a GPR model g_n for the performance function g using the training dataset $\boldsymbol{\mathcal{D}}$. This is accomplished in the present study with the *fitrgp* function from the Statistics and Machine Learning Toolbox of Matlab R2024a, with a constant prior mean and an anisotropic Gaussian kernel for the prior covariance. The involved hyper-parameters are solved by maximizing the log-marginal likelihood with the quasi-Newton method.

Step 5: Calculate the three terms $\hat{P}_{f,n}(t_0, t_f)$, $\hat{P}^{+}_{f,n}(t_0, t_f)$ and $\hat{P}^{-}_{f,n}(t_0, t_f)$

Calculate the time-dependent failure probability estimate $\hat{P}_{f,n}(t_0, t_f)$ via MCS with $\boldsymbol{S}$, as well as $\hat{P}^{+}_{f,n}(t_0, t_f)$ and $\hat{P}^{-}_{f,n}(t_0, t_f)$.

Step 6: Check the stopping criterion #1

If the stopping criterion $\frac{\hat{P}^{+}_{f,n}(t_0,t_f) - \hat{P}^{-}_{f,n}(t_0,t_f)}{\hat{P}_{f,n}(t_0,t_f)} < \epsilon_3$ is satisfied twice in a row, then go to **Step 8**; otherwise, proceed to **Step 7**.

Step 7: Enrich the training dataset

First, calculate $\widehat{\text{ILCB}}$, $\widehat{\text{IPI}}$ or $\widehat{\text{IEI}}$ via MCS with $\boldsymbol{S}$. Second, identify the next best time instant $t^{(n+1)}$ via Eq. (19), Eq. (22) or Eq. (25). Third, identify the next best point $\left\{\boldsymbol{x}^{(n+1)}, \hat{\boldsymbol{y}}^{(n+1)}(t^{(n+1)})\right\}$ using the learning function L_3 via Eq. (27). Fourth, obtain $z^{(n+1)}$ by evaluating the performance function g at $\boldsymbol{u}^{(n+1)} = \left\{\boldsymbol{x}^{(n+1)}, \hat{\boldsymbol{y}}^{(n+1)}(t^{(n+1)}), t^{(n+1)}\right\}$. Finally, enrich the existing training dataset with the new data, i.e., $\boldsymbol{\mathcal{D}} = \boldsymbol{\mathcal{D}} \cup \left\{\boldsymbol{u}^{(n+1)}, z^{(n+1)}\right\}$. Let $n = n + 1$ and go to **Step 4**.

Step 8: Check the stopping criterion #2

First, calculate the CoV of $\hat{P}_{f,n}(t_0, t_f)$, denoted as $\text{CoV}\left[\hat{P}_{f,n}(t_0, t_f)\right]$. Then, if $\text{CoV}\left[\hat{P}_{f,n}(t_0, t_f)\right] < \eta$ is satisfied (η is a user-specified threshold), proceed to **Step 10**; otherwise, continue to **Step 9**. Note that

this stopping criterion ensures that the sample size of MCS is sufficient to maintain the sampling variability below an acceptable level for estimating the time-dependent failure probability.

Step 9: Enrich the sample pool

First, generate an additional sample $\boldsymbol{S}^+$ like in **Step 2**. Then, enrich the existing sample pool with the new sample, i.e., $\boldsymbol{S} = \boldsymbol{S} \cup \boldsymbol{S}^+$, and proceed to **Step 5**.

Step 10: Return the time-dependent failure probability

Return $\hat{P}_{f,n}(t_0, t_f)$ as the final result of the time-dependent failure probability.

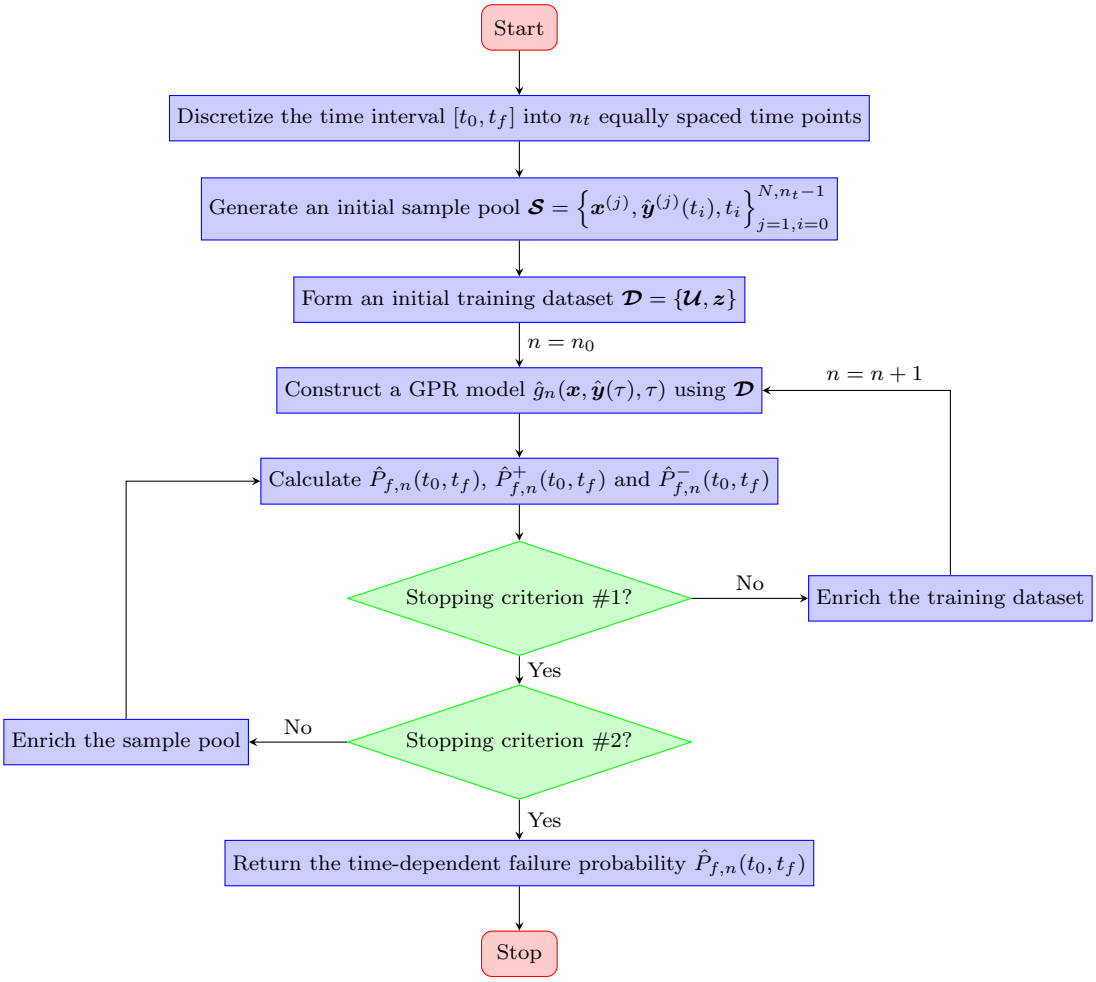

Figure 2: Flowchart of the proposed IBIO method.

Remark 3. The proposed method is designed for the general case where the time-dependent performance function takes the form $g(\boldsymbol{X}, \boldsymbol{Y}(t), t)$. As a result, it is also applicable to special cases such as $g(\boldsymbol{X}, t)$,

$g(\boldsymbol{Y}(t))$, $g(\boldsymbol{Y}(t), t)$ and $g(\boldsymbol{X}, \boldsymbol{Y}(t))$.

Remark 4. In addition to the time-dependent failure probability $\hat{P}_{f,n}(t_0, t_f)$, the time-dependent failure probability function $\hat{P}_{f,n}(t_0, t)$ for $t \in [t_0, t_f]$ can also be obtained as a by-product of the proposed method. For example, $\hat{P}_f(t_0, t_l)$ for $l = 0, 1, \cdots, n_t - 2$ can be achieved by simply replacing $n_t - 1$ with l in the right-hand side of Eq. (9).

4. Numerical examples

In this section, five numerical examples are provided to demonstrate the effectiveness of the proposed IBIO method for time-dependent reliability analysis. The parameters of the proposed method are set as follows: $N = 10^5$, $n_0 = 10$, $\delta = 99.5\%$, $b = 1.25$, $\epsilon_3 = 10\%$ and $\eta = 2\%$. Note that the IBIO method is further labeled as IBIO-ILCB, IBIO-IPI, and IBIO-IEI to indicate the learning function used to identify the optimal next time instant. For comparison, several existing methods (i.e., eSPT [43], SILK [23], AFPK [24] and REAL [26]) are included where applicable. To evaluate robustness, these methods, along with the proposed methods, are each run 20 independent times when the results are generated by us. All simulations are conducted on a MacBook Pro (14-inch, November 2023) equipped with an Apple M3 chip, 24 GB of RAM, and running macOS Sonoma 14.5.

4.1. Example 1: A benchmark problem

The first numerical example considers a benchmark problem adopted from [43]:

$$g(\boldsymbol{X}, Y(t), t) = X_1^2 X_2 - 5X_1(1 + Y(t))t + (X_2 + 1)\, t^2 - 20, \tag{30}$$

where $t \in [0, 1]$; X_1 and X_2 are two random variables, $Y(t)$ is a stochastic process, as detailed in Table 1. The time interval $[0, 1]$ is discretized into 50 equally spaced time points.

Table 2 compares the performance of various methods for estimating the time-dependent failure probability $P_f(0, 1)$. The reference failure probability is adopted as 0.3081 (with a negligible CoV of 0.05%), which is given by MCS with 50×10^7 performance function evaluations. The proposed IBIO methods deliver comparable failure probability means with small CoVs (0.35% - 0.63%), yet require on average fewer than

Table 1: Random variables and stochastic process of Example 1.

Symbol	Distribution	Mean	Standard deviation	Auto-correlation coefficient
X_1	Normal	3.50	0.25	-
X_2	Normal	3.50	0.25	-
$Y(t)$	Gaussian process	0	1	$\exp\left(-(t_2-t_1)^2\right)$

14 evaluations of the g function. In contrast, other methods (i.e., eSPT, SILK, AFPK and REAL) incur higher computational cost in terms of g-function evaluations, and exhibit slightly larger CoVs in their failure probability estimates.

Table 2: Time-dependent failure probability results of Example 1.

Method	N_{call}		$\hat{P}_f(0,1)$		Reference
	Mean	CoV	Mean	CoV	
MCS	50×10^7	-	0.3081	0.05%	-
eSPT	51.9	-	0.3082	1.52%	[24]
SILK	25.7	-	0.3094	4.03%	[24]
AFPK	24.4	-	0.3084	2.98%	[24]
REAL	21.75	-	0.3093	3.21%	[30]
Proposed IBIO-ILCB	13.20	3.11%	0.3089	0.35%	-
Proposed IBIO-IPI	13.60	4.40%	0.3081	0.63%	-
Proposed IBIO-IEI	13.25	3.35%	0.3088	0.43%	-

Note: N_{call} = the number of calls to the g-function;

Fig. 3 depicts the statistical results of the time-dependent failure probability function $\hat{P}_f(0,t)$ for $t \in [0,1]$, obtained through post-processing the proposed IBIO methods, in comparison to the reference result generated by MCS. As seen, the mean curves closely align with the reference, while the mean $\pm$ standard deviation (Std Dev) bands remain notably narrow.

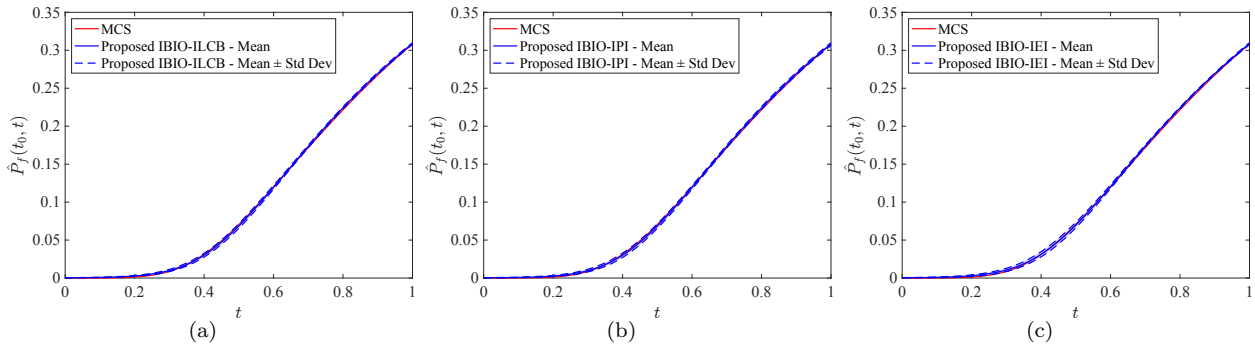

Figure 3: Time-dependent failure probability function for Example 1.

4.2. Example 2: A simple supported beam

The second example involves a simple supported steel beam [2], as shown in Fig. 4. The beam has a length of $L = 5$ m, and a rectangular cross section with an initial width b_0 and height h_0. The cross section undergoes isotropic corrosion over time at a constant rate of $2k$, where $k = 3 \times 10^{-5}$ m. The yield stress of the steel material is denoted as f_y. The beam is subjected to a live concentrated load $F(t)$ at its mid-span, along with a uniform dead load $q = 78500 b_0 h_0$. The time-dependent performance function is given by:

$$g(\boldsymbol{X}, Y(t), t) = \frac{(b_0 - 2kt)(h_0 - 2kt)^2 f_y}{4} - \left(\frac{F(t)L}{4} + \frac{78500 b_0 h_0 L^2}{8}\right), \tag{31}$$

where $t \in [0, 10]$ year; b_0, h_0 and f_y are three random variables and $F(t)$ is a stochastic process, as described in Table 3. The time period $[0, 10]$ is discretized into 300 time nodes.

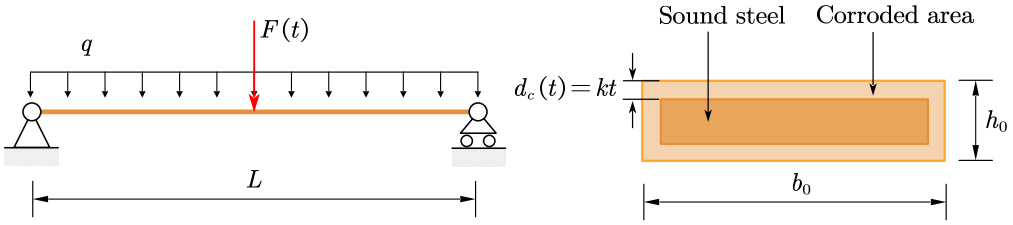

Figure 4: A simple supported beam.

The results of various methods are summarized in Table 4. The reference time-dependent failure probability obtained using MCS is 7.71×10^{-3}, with a very small CoV of 0.51%. However, this comes at the cost of an exceptionally large computational effort, requiring $300 \times 5 \times 10^6$ performance function evaluations. The

Table 3: Random variables and stochastic process of Example 2.

Symbol	Distribution	Mean	Standard deviation	Auto-correlation coefficient
f_y (MPa)	Lognormal	180	18	-
b_0 (m)	Lognormal	0.2	0.01	-
h_0 (m)	Lognormal	0.04	0.004	-
$F(t)$ (N)	Gaussian process	3500	700	$\exp\left(-9(t_2-t_1)^2\right)$

eSPT, SILK, AFPK, and REAL methods provide reasonable mean values for the failure probability estimates with moderate computational effort, requiring an average of 23.20 to 59.33 g-function calls. All IBIO methods require fewer than 19 performance function evaluations on average, outperforming other methods while providing reasonable failure probability estimates.

Table 4: Time-dependent failure probability results of Example 2.

Method	N_{call}		$\hat{P}_f(0,10)$		Reference
	Mean	CoV	Mean	CoV	
MCS	$300 \times 5 \times 10^6$	-	7.71×10^{-3}	0.51%	-
eSPT	59.33	-	7.68×10^{-3}	1.61%	[29]
SILK	44.67	-	7.75×10^{-3}	1.60%	[29]
AFPK	23.20	-	7.79×10^{-3}	1.60%	[29]
REAL	32.30	9.21%	7.75×10^{-3}	2.35%	-
Proposed IBIO-ILCB	17.70	8.22%	7.67×10^{-3}	2.28%	-
Proposed IBIO-IPI	18.90	7.85%	7.65×10^{-3}	3.78%	-
Proposed IBIO-IEI	18.45	11.32%	7.70×10^{-3}	5.72%	-

The statistical results of the time-dependent failure probability function $\hat{P}(0,t)$ for $t \in [0,10]$ obtained from the proposed methods are depicted in Fig. 5, along with the reference provided by MCS. It is shown that the mean curves agree well with the reference and the mean $\pm$ std dev bands are narrow.

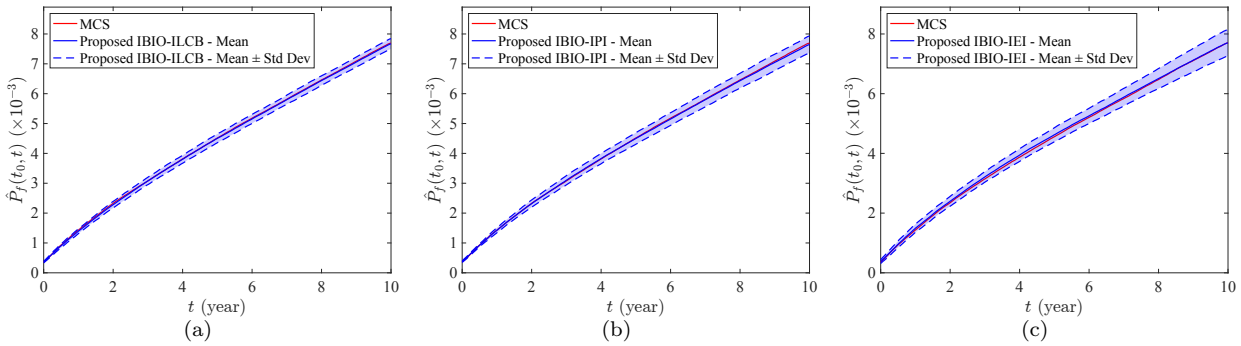

Figure 5: Time-dependent failure probability function for Example 2.

4.3. Example 3: A cantilever tube

As shown in Fig. 6, this example considers a cantilever tube structure that has been studied extensively [40, 44, 45]. This structure is subject to three forces F_1, F_2 and P, as well as a torque $T(t)$. The yield strength of the material degrades linearly over time $s(t) = s_0(1-0.01t)$, where s_0 is the initial yield strength. The time-dependent performance function is defined as:

$$g(\boldsymbol{X}, Y(t), t) = s(t) - \sqrt{\sigma_x^2 + 3\tau_{zx}^2(t)}, \tag{32}$$

where $t \in [0, 5]$ year; σ_x and $\tau_{zx}(t)$ are given by:

$$\sigma_x = \frac{P + F_1 \sin\theta_1 + F_2 \sin\theta_2}{\frac{\pi}{4}\left[d^2 - (d-2h)^2\right]} + \frac{(F_1 L_1 \cos\theta_1 + F_2 L_2 \cos\theta_2)\, d}{2 \times \frac{\pi}{64}\left[d^4 - (d-2h)^4\right]}, \tag{33}$$

$$\tau_{zx}(t) = \frac{T(t) d}{4 \times \frac{\pi}{64}\left[d^4 - (d-2h)^4\right]}, \tag{34}$$

in which $\theta_1 = 5°$, $\theta_2 = 10°$, $L_1 = 120$ mm and $L_2 = 60$ mm; F_1, F_2, P, h, d and s_0 are six random variables, and $T(t)$ is a stochastic process, as reported in Table 5. In this example, the time interval $[0, 5]$ is discretized into 100 time nodes.

Table 6 summarizes the results obtained using different methods, including MCS, SILK, REAL, IBIO-ILCB, IBIO-IPI, and IBIO-IEI. The reference failure probability provided by MCS is 1.36×10^{-2}, with a CoV of 0.85%, achieved at the expense of 100×10^6 performance function calls. SIlK can produce a failure probability mean close to the reference, while a relatively small CoV of 2.19%, requiring an average of 71.00 g-function evaluations. REAL reduces the average number of g-function evaluations to just 13.40,

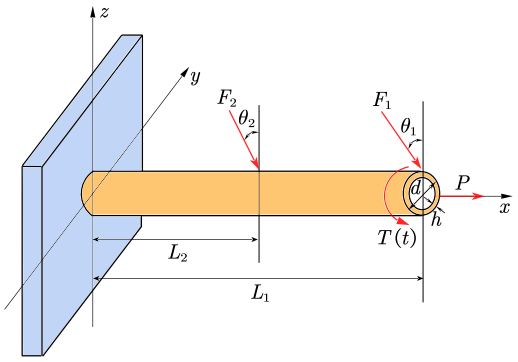

Figure 6: A cantilever tube subject to three forces and one torque.

Table 5: Random variables and stochastic process of Example 3.

Symbol	Distribution	Mean	CoV	Auto-correlation coefficient
F_1 (N)	Normal	1800	0.10	-
F_2 (N)	Normal	1800	0.10	-
P (N)	Lognormal	1000	0.10	-
h (mm)	Normal	5	0.019	-
d (mm)	Normal	42	0.02	-
s_0 (MPa)	Normal	500	0.10	-
$T(t)$ (N $\cdot$ mm)	Gaussian process	1.7×10^6	0.10	$\exp\left(-4(t_2 - t_1)^2\right)$

albeit with a relatively high CoV of 26.35%. However, its failure probability estimates exhibit significant variability, as indicated by a CoV of 16.47%, even though the mean value remains close to the reference result. Compared to SILK and REAL, all IBIO methods strike a more favorable balance between efficiency and accuracy. However, it is worth noting that the number of performance function evaluations exhibits a high CoV for IBIO-ILCB.

Fig. 7 presents the statistical results of the time-dependent failure probability function $\hat{P}_f(0,t)$ for $t \in [0,5]$ obtained using the proposed IBIO methods, alongside the reference result from MCS. It is evident that the mean value curves for all IBIO methods closely approximate the MCS reference solution, with narrow mean $\pm$ std dev bands.

Table 6: Time-dependent failure probability results of Example 3.

Method	N_{call}		$\hat{P}_f(0,5)$	
	Mean	CoV	Mean	CoV
MCS	100×10^6	-	1.36×10^{-2}	0.85%
SILK	71.00	11.30%	1.36×10^{-2}	2.19%
REAL	13.40	26.35%	1.35×10^{-2}	16.47%
Proposed IBIO-ILCB	20.25	21.55%	1.35×10^{-2}	3.54%
Proposed IBIO-IPI	18.85	10.51%	1.33×10^{-2}	3.31%
Proposed IBIO-IEI	18.30	8.14%	1.35×10^{-2}	3.68%

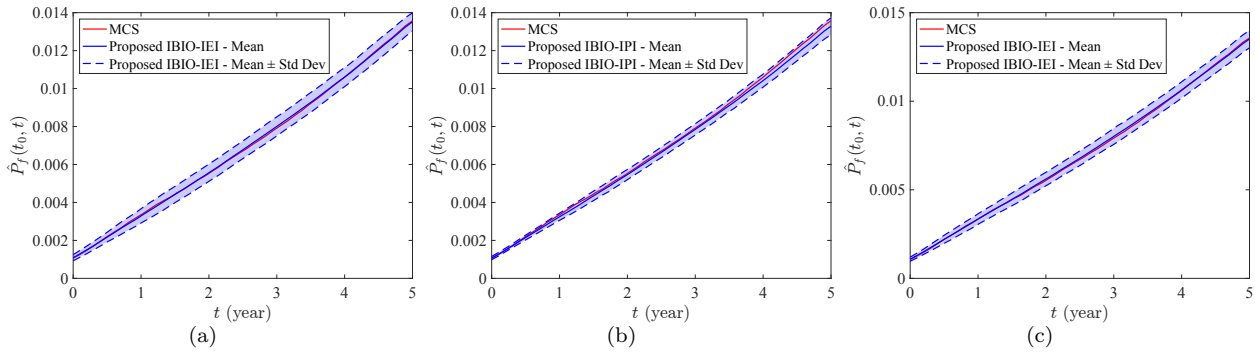

Figure 7: Time-dependent failure probability function for Example 3.

4.4. Example 4: A spatial truss structure

The fourth numerical example involves a 120-bar spatial truss structure under thirteen vertical concentrated loads [37], as shown in Fig. 8. The structure is modeled as a three-dimensional finite element model using the open-source software framework OpenSees (https://opensees.berkeley.edu/). The model consists of 49 nodes and 120 truss elements. It is assumed that all the elements have the same cross-sectional area A and young's modulus E. A time-varying vertical concentrated load $P_0(t)$ is applied to node 0, while 12 static vertical concentrated loads $P_1, P_2, \cdots, P_{12}$ are applied to nodes 1 through 12. The time-dependent performance function is defined as:

$$g(\boldsymbol{X}, Y(t)) = \Delta - V_0(E, A, P_0(t), P_1, P_2, \cdots, P_{12}), \tag{35}$$

where $t \in [0, 50]$ year; V_0 denotes the vertical displacement of node 0 along the negative of z-axis; Δ represents the allowable displacement, which is set to 100 mm; E, A, $P_0(t)$, P_1, P_2, $\cdots$ and P_{12} are given in Table 7. The time period $[0, 50]$ is discretized into 20 time nodes.

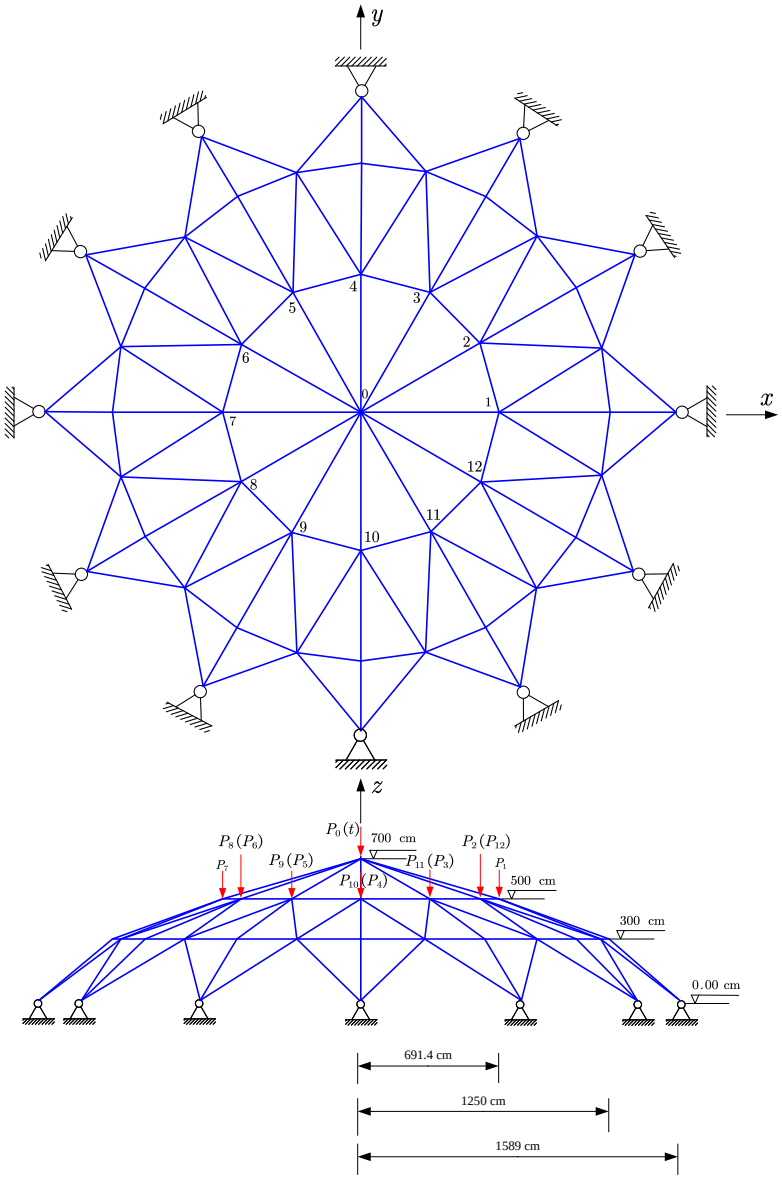

Figure 8: A 120-bar spatial truss structure under vertical loads.

Table 8 presents the results of various methods for estimating the time-dependent failure probability, $\hat{P}_f(0, 50)$. The reference value of the failure probability is taken as 2.81×10^{-2} (with a CoV of 0.83%), which

Table 7: Random variables and stochastic process of Example 4.

Symbol	Distribution	Mean	CoV	Auto-correlation coefficient
E (GPa)	Normal	200	0.10	-
A (mm^2)	Normal	2000	0.10	-
$P_1, P_2, \cdots, P_{12}$ (kN)	Lognormal	100	0.15	-
$P_0(t)$ (kN)	Lognormal process	1000	0.15	$\exp\left(-(t_2 - t_1)^2/50\right)$

Note: The auto-correlation coefficient function for $P_0(t)$ is defined for the underlying Gaussian process.

is provided by MCS with $20 \times 5 \times 10^5$ model evaluations (taking 34,808.18 s $\approx$ 9.67 h). The results for both SILK and REAL are unavailable as they fail to meet their stopping criteria before encountering memory limitations. All the proposed IBIO methods provide reasonably accurate results for the failure probability, requiring only about 37 model evaluations and 34.45 - 36.67 s on average. It is worth noting that the number of model evaluations for IBIO-ILCB exhibits slightly large variability.

Table 8: Time-dependent failure probability results of Example 4.

Method	N_{call}		$\hat{P}_f(0, 50)$		Time (s)	
	Mean	CoV	Mean	CoV	Mean	CoV
MCS	$20 \times 5 \times 10^5$	-	2.81×10^{-2}	0.83%	34,808.19	-
SILK	-	-	-		-	-
REAL	-	-	-		-	-
Proposed IBIO-ILCB	37.40	18.91%	2.83×10^{-2}	2.46%	34.73	-
Proposed IBIO-IPI	36.95	13.13%	2.83×10^{-2}	2.65%	36.67	-
Proposed IBIO-IEI	36.85	11.08%	2.82×10^{-2}	2.06%	34.45	-

Fig. 9 depicts the statistical results of the failure probability function $\hat{P}_f(0, t)$ for $t \in [0, 50]$ obtained using the proposed IBIO methods, alongside the reference curve provided by MCS. It can be observed that:

(1) the mean value curves by the proposed methods accord well with the reference one; (2) the mean ± std dev bands are rather narrow.

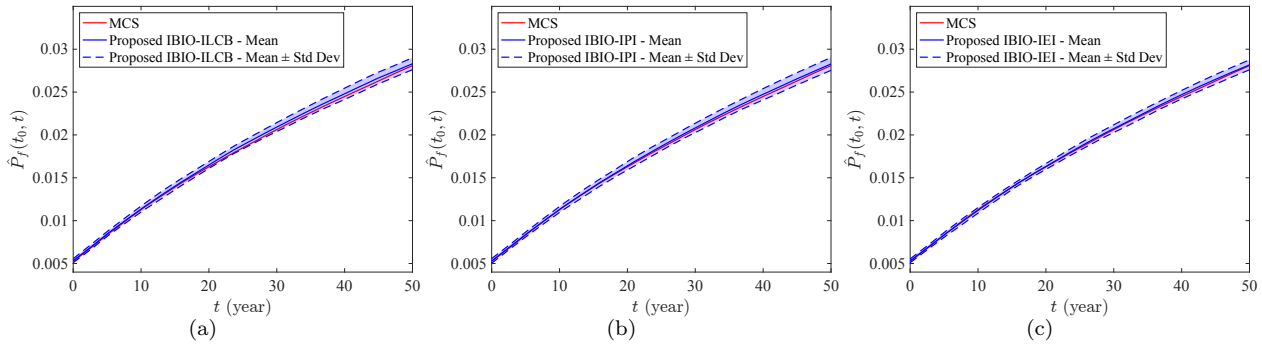

Figure 9: Time-dependent failure probability function for Example 4.

4.5. Example 5: A rigid-frame bridge structure

As a final example, we consider a three-span rigid-frame bridge structure, which is shown in Fig. 10(a). The bridge spans a total length of 60 m, divided into three equal 20 m spans, and featuring a constant deck width of 6 m. The deck thickness varies linearly from 1 m at the end supports to 2 m at the pier locations. Two rectangular piers — each 3 m wide, 6 m long, and 10 m high — are positioned at the 20 m and 40 m marks along the deck. A three-dimensional finite-element model is built in MATLAB's PDE Toolbox (Fig. 10(b)), with fixed boundary conditions applied to the deck's end faces and the piers' base faces, and a uniform vertical load $Q(t)$ imposed on the deck's top surface. The Young's moduli of the deck and piers degrade over time following $E_d(t) = E_{d,0}(1 - \gamma \log(1 + t))$ and $E_p(t) = E_{p,0}(1 - \gamma \log(1 + t))$, where $E_{d,0}$ and $E_{p,0}$ are the initial Young's modulus and $\gamma = 0.05$ is adopted in this study. Both deck and piers share a Poisson's ratio of 0.20. The time-dependent performance function is defined as:

$$g(\boldsymbol{X}, Y(t), t) = \Delta - V_m(E_{d,0}, E_{p,0}, Q(t), t), \tag{36}$$

where $t \in [0, 5]$ year; V_m denotes the vertical deflection of the deck at mid-span; Δ is the maximum allowable deflection, which is specified as 0.05 m. The involved random variables and stochastic process are listed in Table 9. The time period $[0, 5]$ is discretized into 20 time nodes.

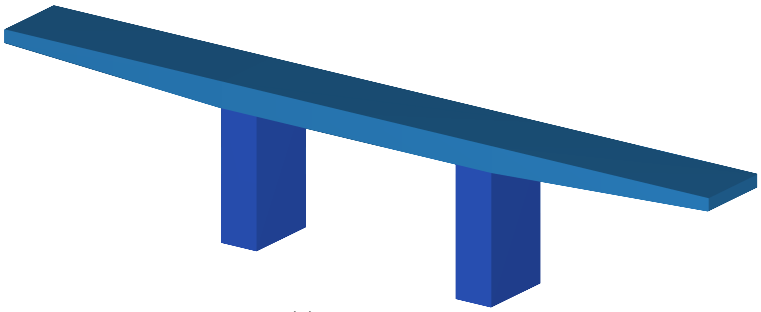

(a)

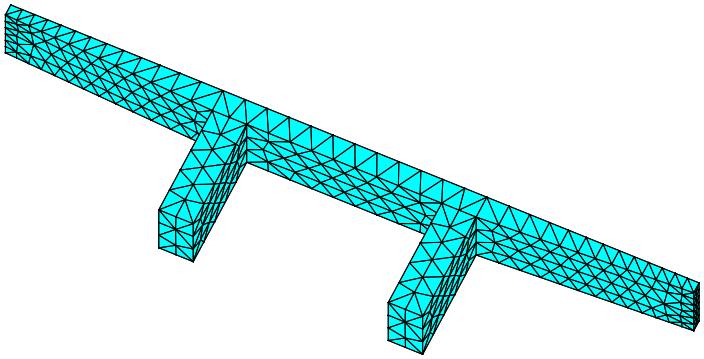

(b)

Figure 10: A rigid-frame bridge structure: (a) Schematic diagram; (b) Finite-element mesh.

Table 10 presents the results obtained with different methods. Since a full MCS is computationally infeasible for this example, we adopt the mean value of the time-dependent failure probabilities from the SILK method as the reference. The reference value is 8.62×10^{-2} with a CoV of 0.83%, achieved at an average cost of 32.80 model evaluations and 27.95 s. The REAL exhibits large variability for the number of model evaluations (a CoV up to 20.90%), and also for the time-dependent failure probabilities (a CoV of 9.84%). Furthermore, the mean value of time-dependent failure probabilities deviates markedly from the reference. By contrast, all the proposed IBIO methods show reasonable variability and yield mean failure

Table 9: Random variables and stochastic process of Example 5.

Symbol	Distribution	Mean	Standard deviation	Auto-correlation coefficient
$E_{d,0}$	Lognormal	30 GPa	3.0 GPa	-
$E_{p,0}$	Lognormal	35 GPa	3.5 GPa	-
$Q(t)$	Gaussian process	1000 kN/m^2	150 kN/m^2	$\exp\left(-\lvert t_2 - t_1\rvert/25\right)$

probabilities that closely match the reference. Note that these methods only require an average of about 16 performance function calls and 5 seconds to run, which is far less than SILK.

Table 10: Time-dependent failure probability results of Example 5.

Method	N_{call}		$\hat{P}_f(0,5)$		Time (s)	
	Mean	CoV	Mean	CoV	Mean	CoV
SILK	32.80	12.73%	8.62×10^{-2}	0.83%	27.95	-
REAL	15.90	20.90%	8.26×10^{-2}	9.84%	6.46	-
Proposed IBIO-ILCB	15.65	6.31%	8.71×10^{-2}	0.79%	4.74	-
Proposed IBIO-IPI	15.70	5.51%	8.73×10^{-2}	1.34%	4.90	-
Proposed IBIO-IEI	16.10	8.99%	8.73×10^{-2}	1.08%	4.95	-

The statistical results of the time-dependent failure probability function $\hat{P}_f(0,t)$ for $t \in [0,5]$ are shown in Fig. 11, together with the reference from SILK. It can be seen that the mean $\pm$ std dev bounds are quite narrow and the mean curves are close to the reference.

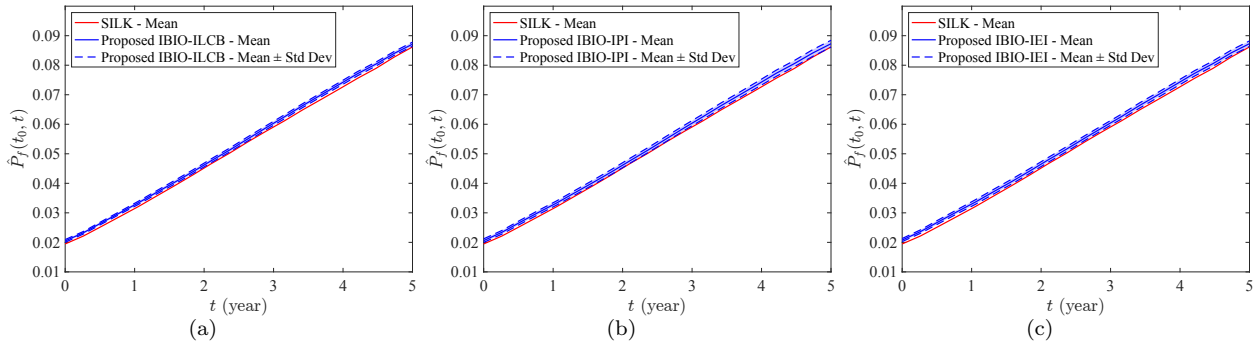

Figure 11: Time-dependent failure probability function for Example 5.

5. Concluding remarks

This paper presents a novel single-loop Bayesian active learning method for computationally expensive time-dependent reliability analysis, called 'Integrated Bayesian integration and Optimization' (IBIO). The underlying idea is to construct a computationally efficient Gaussian process regression model to replace the original expensive-to-evaluate performance function, leveraging a Bayesian active learning approach. This is achieved by ingeniously integrating the Bayesian probabilistic integration for static reliability analysis and the Bayesian global optimization for finding the global optima of expensive black-box functions. Specifically, we first introduce a pragmatic estimator for the time-dependent failure probability. Based on this estimator, a novel stopping criterion is then proposed to determine when to terminate the active learning processes. Furthermore, new learning functions are also proposed to identify the promising point where to evaluate the true performance function next when the stopping criterion is not reached. More precisely, three alternative learning functions are formulated to select the next optimal time instant from a Bayesian optimization perspective, but in an average sense. In addition, another learning function, adapted from one Bayesian integration method for static reliability analysis, is introduced to guide the selection of the next optimal sample for random variables and stochastic processes at the identified time instant. The proposed method is applicable whether or not the performance function is subject to stochastic processes. Besides, it can provide not only the time-dependent failure probability over the reference time interval, but also the evolution of the failure probability over the interval as a by-product. Numerical results indicate that the proposed method can significantly reduce the number of performance function evaluations while maintaining high accuracy. In addition, none of the three proposed learning functions for selecting the next optimal time instant consistently and significantly outperforms the others.

While the proposed method exhibits considerable strengths, several avenues for future improvement remain. First, extending the approach to high-dimensional problems remains a significant task. Second, accurately estimating very small failure probabilities will likely demand more efficient techniques than crude MCS.

CRediT authorship contribution statement

Chao Dang: Conceptualization, Methodology, Software, Validation, Investigation, Writing - Original Draft, Visualization. **Marcos A. Valdebenito:** Conceptualization, Validation, Writing - Review & Editing, Supervision. **Matthias G.R. Faes:** Resources, Writing - Review & Editing, Supervision, Project administration, Funding acquisition.

Declaration of competing interest

The authors declare that they have no known competing financial interests or personal relationships that could have appeared to influence the work reported in this paper.

Acknowledgments

Chao Dang is grateful for the financial support of the German Research Foundation (DFG) (Grant number 530326817).

Data availability

No data was used for the research described in the article.

Appendix A. Brief introduction to Gaussian process regression

For notational simplicity, we denote the input of the performance function as $\boldsymbol{u}$ and the corresponding output as z, i.e., $\boldsymbol{u} = [\boldsymbol{x}, \hat{\boldsymbol{y}}(t), t]$ and $z = g(\boldsymbol{u})$. GPR places a GP prior over the performance function:

$$g_0(\boldsymbol{u}) \sim \mathcal{GP}(m_{g_0}(\boldsymbol{u}), k_{g_0}(\boldsymbol{u}, \boldsymbol{u}')), \tag{A.1}$$

where g_0 denotes the prior distribution of g before seeing any observations; m_{g_0} and k_{g_0} are the prior mean and covariance functions, respectively.

Given a dataset of n observations, $\boldsymbol{\mathcal{D}} = \{\boldsymbol{\mathcal{U}}, \boldsymbol{z}\}$, where $\boldsymbol{\mathcal{U}}$ is an n-by-$(d_1 + d_2 + 1)$ matrix with its i-th row being $\boldsymbol{u}^{(i)}$ and $\boldsymbol{z}$ is an n-by-1 vector with its i-th element being $z^{(i)} = g(\boldsymbol{u}^{(i)})$ for $i = 1, 2, \cdots, n$, conditioning this dataset on the prior distribution gives rise to a GP posterior for the performance function:

$$g_n(\boldsymbol{u}) \sim \mathcal{GP}(m_{g_n}(\boldsymbol{u}), k_{g_n}(\boldsymbol{u}, \boldsymbol{u}')), \tag{A.2}$$

where g_n denotes the posterior distribution of g after seeing n observations; m_{g_n} and k_{g_n} are the posterior mean and covariance functions respectively, which are given by:

$$m_{g_n}(\boldsymbol{u}) = m_{g_0}(\boldsymbol{u}) + \boldsymbol{k}_{g_0}(\boldsymbol{u}, \boldsymbol{\mathcal{U}})^\top \boldsymbol{K}_{g_0}^{-1}(\boldsymbol{z} - \boldsymbol{m}_{g_0}(\boldsymbol{\mathcal{U}})), \tag{A.3}$$

$$k_{g_n}(\boldsymbol{u}, \boldsymbol{u}') = k_{g_0}(\boldsymbol{u}, \boldsymbol{u}') - \boldsymbol{k}_{g_0}(\boldsymbol{u}, \boldsymbol{\mathcal{U}})^\top \boldsymbol{K}_{g_0}^{-1} \boldsymbol{k}_{g_0}(\boldsymbol{\mathcal{U}}, \boldsymbol{u}'), \tag{A.4}$$

where $\boldsymbol{m}_{g_0}(\boldsymbol{\mathcal{U}})$ is an n-by-1 vector with its i-th element being $m_{g_0}(\boldsymbol{u}^{(i)})$; $\boldsymbol{k}_{g_0}(\boldsymbol{u}, \boldsymbol{\mathcal{U}})$ and $\boldsymbol{k}_{g_0}(\boldsymbol{\mathcal{U}}, \boldsymbol{u}')$ are two n-by-1 vectors with their i-th elements being $k_{g_0}(\boldsymbol{u}, \boldsymbol{u}^{(i)})$ and $k_{g_0}(\boldsymbol{u}^{(i)}, \boldsymbol{u}')$, respectively; $\boldsymbol{K}_{g_0}$ is an n-by-n matrix with its entry being $k_{g_0}(\boldsymbol{u}^{(i)}, \boldsymbol{u}^{(j)})$.

References

[1] S. O. Rice, Mathematical analysis of random noise, The Bell System Technical Journal 23 (3) (1944) 282–332. doi:10.1002/j.1538-7305.1944.tb00874.x.

[2] C. Andrieu-Renaud, B. Sudret, M. Lemaire, The PHI2 method: a way to compute time-variant reliability, Reliability Engineering & System Safety 84 (1) (2004) 75–86. doi:https://doi.org/10.1016/j.ress.2003.10.005.

[3] B. Sudret, Analytical derivation of the outcrossing rate in time-variant reliability problems, Structure and Infrastructure Engineering 4 (5) (2008) 353–362. doi:https://doi.org/10.1080/15732470701270058.

[4] X.-Y. Zhang, Z.-H. Lu, S.-Y. Wu, Y.-G. Zhao, An efficient method for time-variant reliability including finite element analysis, Reliability Engineering & System Safety 210 (2021) 107534. doi:https://doi.org/10.1016/j.ress.2021.107534.

[5] B. Zhang, W. Wang, H. Lei, X. Hu, C.-Q. Li, An improved analytical solution to outcrossing rate for scalar nonstationary and non-Gaussian processes, Reliability Engineering & System Safety 247 (2024) 110102. doi:https://doi.org/10.1016/j.ress.2024.110102.

[6] C.-Q. Li, A. Firouzi, W. Yang, Closed-form solution to first passage probability for nonstationary lognormal processes, Journal of Engineering Mechanics 142 (12) (2016) 04016103. doi:https://doi.org/10.1061/(ASCE)EM.1943-7889.0001160.

[7] A. Firouzi, W. Yang, C.-Q. Li, Efficient solution for calculation of upcrossing rate of nonstationary Gaussian process, Journal of Engineering Mechanics 144 (4) (2018) 04018015. doi:https://doi.org/10.1061/(ASCE)EM.1943-7889.0001420.

[8] W. Yang, B. Zhang, W. Wang, C.-Q. Li, Time-dependent structural reliability under nonstationary and non-Gaussian processes, Structural Safety 100 (2023) 102286. doi:https://doi.org/10.1016/j.strusafe.2022.102286.

[9] C. Jiang, X. Huang, X. Han, D. Zhang, A time-variant reliability analysis method based on stochastic process discretization, Journal of Mechanical Design 136 (9) (2014) 091009. doi:https://doi.org/10.1115/1.4027865.

[10] Z. P. Mourelatos, M. Majcher, V. Pandey, I. Baseski, Time-dependent reliability analysis using the total probability theorem, Journal of Mechanical Design 137 (3) (2015) 031405. doi:https://doi.org/10.1115/1.4029326.

[11] C. Gong, D. M. Frangopol, An efficient time-dependent reliability method, Structural Safety 81 (2019) 101864. doi:https://doi.org/10.1016/j.strusafe.2019.05.001.

[12] X. Yuan, W. Zheng, C. Zhao, M. A. Valdebenito, M. G. Faes, Y. Dong, Line sampling for time-variant failure probability estimation using an adaptive combination approach, Reliability Engineering & System Safety 243 (2024) 109885. doi:https://doi.org/10.1016/j.ress.2023.109885.

[13] X. Yuan, S. Liu, M. Faes, M. A. Valdebenito, M. Beer, An efficient importance sampling approach for reliability analysis of time-variant structures subject to time-dependent stochastic load, Mechanical Systems and Signal Processing 159 (2021) 107699. doi:https://doi.org/10.1016/j.ymssp.2021.107699.

[14] X. Yuan, Y. Shu, Y. Qian, Y. Dong, Adaptive importance sampling approach for structural time-variant reliability analysis, Structural Safety 111 (2024) 102500. doi:https://doi.org/10.1016/j.strusafe.2024.102500.

[15] H.-S. Li, T. Wang, J.-Y. Yuan, H. Zhang, A sampling-based method for high-dimensional time-variant reliability analysis, Mechanical Systems and Signal Processing 126 (2019) 505–520. doi:https://doi.org/10.1016/j.ymssp.2019.02.050.

[16] M. Ping, X. Han, C. Jiang, X. Xiao, A time-variant extreme-value event evolution method for time-variant reliability analysis, Mechanical Systems and Signal Processing 130 (2019) 333–348. doi:https://doi.org/10.1016/j.ymssp.2019.05.009.

[17] Y. Zhang, J. Xu, M. Beer, A single-loop time-variant reliability evaluation via a decoupling strategy and probability distribution reconstruction, Reliability Engineering & System Safety 232 (2023) 109031. doi:https://doi.org/10.1016/j.ress.2022.109031.

[18] Y. Zhang, J. Xu, P. Gardoni, A loading contribution degree analysis-based strategy for time-variant reliability analysis of structures under multiple loading stochastic processes, Reliability Engineering & System Safety 243 (2024) 109833. doi:https://doi.org/10.1016/j.ress.2023.109833.

[19] Z. Wang, P. Wang, A new approach for reliability analysis with time-variant performance characteristics, Reliability Engineering & System Safety 115 (2013) 70–81.

[20] Z. Hu, X. Du, Mixed efficient global optimization for time-dependent reliability analysis, Journal of Mechanical Design 137 (5) (2015) 051401. doi:https://doi.org/10.1115/1.4029520.

[21] J. Wu, Z. Jiang, H. Song, L. Wan, F. Huang, Parallel efficient global optimization method: a novel approach for time-dependent reliability analysis and applications, Expert Systems with Applications 184 (2021) 115494. doi:https://doi.org/10.1016/j.eswa.2021.115494.

[22] H. Li, Z. Lu, K. Feng, A double-loop Kriging model algorithm combined with importance sampling for time-dependent reliability analysis, Engineering with Computers 40 (3) (2024) 1539–1558. doi:https://doi.org/10.1007/s00366-023-01879-8.

[23] Z. Hu, S. Mahadevan, A single-loop Kriging surrogate modeling for time-dependent reliability analysis, Journal of Mechanical Design 138 (6) (2016) 061406. doi:https://doi.org/10.1115/1.4033428.

[24] C. Jiang, D. Wang, H. Qiu, L. Gao, L. Chen, Z. Yang, An active failure-pursuing Kriging modeling method for time-dependent reliability analysis, Mechanical Systems and Signal Processing 129 (2019) 112–129. doi:https://doi.org/10.1016/j.ymssp.2019.04.034.

[25] Y. Hu, Z. Lu, N. Wei, C. Zhou, A single-loop Kriging surrogate model method by considering the first failure instant for time-dependent reliability analysis and safety lifetime analysis, Mechanical Systems and Signal Processing 145 (2020) 106963. doi:https://doi.org/10.1016/j.ymssp.2020.106963.

[26] C. Jiang, H. Qiu, L. Gao, D. Wang, Z. Yang, L. Chen, Real-time estimation error-guided active learning Kriging method for time-dependent reliability analysis, Applied Mathematical Modelling 77 (2020) 82–98. doi:https://doi.org/10.1016/j.apm.2019.06.035.

[27] Z. Song, H. Zhang, L. Zhang, Z. Liu, P. Zhu, An estimation variance reduction-guided adaptive Kriging method for efficient time-variant structural reliability analysis, Mechanical Systems and Signal Processing 178 (2022) 109322. doi:https://doi.org/10.1016/j.ymssp.2022.109322.

[28] Y. Lu, Z. Lu, K. Feng, A novel training point selection strategy guided by the maximum reduction of structural state misclassification probability for time-dependent reliability analysis, Aerospace Science and Technology 140 (2023) 108493. doi:https://doi.org/10.1016/j.ast.2023.108493.

[29] D. Wang, H. Qiu, L. Gao, C. Jiang, A subdomain uncertainty-guided Kriging method with optimized feasibility metric for time-dependent reliability analysis, Reliability Engineering & System Safety 243 (2024) 109839. doi:https://doi.org/10.1016/j.ress.2023.109839.

[30] C. Dang, M. A. Valdebenito, M. G. Faes, Towards a single-loop Gaussian process regression based-active learning method for time-dependent reliability analysis, Mechanical Systems and Signal Processing (2025) 112294doi:https://doi.org/10.1016/j.ymssp.2024.112294.

[31] C. Dang, M. G. Faes, M. A. Valdebenito, P. Wei, M. Beer, Partially Bayesian active learning cubature for structural reliability analysis with extremely small failure probabilities, Computer Methods in Applied Mechanics and Engineering 422 (2024) 116828. doi:https://doi.org/10.1016/j.cma.2024.116828.

[32] D. R. Jones, M. Schonlau, W. J. Welch, Efficient global optimization of expensive black-box functions, Journal of Global

Optimization 13 (1998) 455–492. doi:https://doi.org/10.1023/A:1008306431147.

[33] K.-K. Phoon, S. Huang, S. T. Quek, Simulation of second-order processes using karhunen–loeve expansion, Computers & Structures 80 (12) (2002) 1049–1060. doi:https://doi.org/10.1016/S0045-7949(02)00064-0.

[34] C.-C. Li, A. Der Kiureghian, Optimal discretization of random fields, Journal of Engineering Mechanics 119 (6) (1993) 1136–1154. doi:https://doi.org/10.1061/(ASCE)0733-9399(1993)119:6(1136).

[35] J. Zhang, B. Ellingwood, Orthogonal series expansions of random fields in reliability analysis, Journal of Engineering Mechanics 120 (12) (1994) 2660–2677. doi:https://doi.org/10.1061/(ASCE)0733-9399(1994)120:12(2660).

[36] M. Shinozuka, G. Deodatis, Simulation of stochastic processes by spectral representation, Applied Mechanics Reviews 44 (4) (1991) 191–204. doi:https://doi.org/10.1115/1.3119501.

[37] C. Dang, P. Wei, J. Song, M. Beer, Estimation of failure probability function under imprecise probabilities by active learning–augmented probabilistic integration, ASCE-ASME Journal of Risk and Uncertainty in Engineering Systems, Part A: Civil Engineering 7 (4) (2021) 04021054. doi:https://doi.org/10.1061/AJRUA6.0001179.

[38] C. Dang, P. Wei, M. G. Faes, M. A. Valdebenito, M. Beer, Parallel adaptive Bayesian quadrature for rare event estimation, Reliability Engineering & System Safety 225 (2022) 108621. doi:https://doi.org/10.1016/j.ress.2022.108621.

[39] C. Dang, M. A. Valdebenito, M. G. Faes, P. Wei, M. Beer, Structural reliability analysis: A Bayesian perspective, Structural Safety 99 (2022) 102259. doi:https://doi.org/10.1016/j.strusafe.2022.102259.

[40] K. Cheng, Z. Lu, Time-variant reliability analysis based on high dimensional model representation, Reliability Engineering & System Safety 188 (2019) 310–319. doi:https://doi.org/10.1016/j.ress.2019.03.041.

[41] Z. Hu, D. Wang, C. Dang, M. Beer, L. Wang, Uncertainty-aware adaptive Bayesian inference method for structural time-dependent reliability analysis, Reliability Engineering & System Safety, under review (2024).

[42] R. Garnett, Bayesian optimization, Cambridge University Press, 2023.

[43] Z. Wang, W. Chen, Time-variant reliability assessment through equivalent stochastic process transformation, Reliability Engineering & System Safety 152 (2016) 166–175. doi:https://doi.org/10.1016/j.ress.2016.02.008.

[44] Y. Yan, J. Wang, Y. Zhang, Z. Sun, Kriging model for time-dependent reliability: accuracy measure and efficient time-dependent reliability analysis method, IEEE Access 8 (2020) 172362–172378. doi:https://doi.org/10.1109/ACCESS.2020.3014238.

[45] R. Cao, Z. Sun, J. Wang, F. Guo, A single-loop reliability analysis strategy for time-dependent problems with small failure probability, Reliability Engineering & System Safety 219 (2022) 108230. doi:https://doi.org/10.1016/j.ress.2021.108230.